Chaotic Spike Patterns Evoked by Periodic Inhibition of Rat Cortical Neurons

K. A. Schindler, C. A. Bernasconi, R. Stoop, P. H. Goodman, and R. J. Douglas
Institut für Neuroinformatik, ETHZ/UNIZH, Gloriastr. 32, CH-8006 Zürich

Z. Naturforsch. **52a**, 509–512 (1997); received May 13, 1997

We use methods of nonlinear dynamics to describe the effect of periodic inhibition on the patterns of action potentials generated by regular spiking rat cortical neuron *in vitro*. Both direct measurements and our mathematical model reveal that chaotic patterns of discharge can be evoked at certain frequencies of inhibitory stimulation. We use detailed biophysical simulation of a cortical neuron to explain the firing patterns in terms of known membrane ionic conductances.

There is a small voltage difference across the outer membrane of every living cell [1]. Neurons make use of this membrane voltage to perform their computations and to communicate with one another. One very common neuronal communication signal is the action potential, a brief regenerative voltage spike that can travel long distances along the cell membrane without attenuation [2]. The time between spikes (interspike interval duration) may encode information, since the form and distribution of these intervals reflect excitatory and inhibitory signals reaching the nerve cells.

In this paper, we investigate the effect of periodic inhibitory pulses on the output pattern of rat cortical neurons that usually generate a regular train of spikes in response to intracellular injection of a constant stimulating current. The experiments were performed in a brain slice preparation, and also in a simulated cortical pyramidal neuron. We analyze the data using methods of nonlinear dynamics, which are emerging as powerful tools for understanding the behavior of biological systems [3]. We develop and enhance an approach of Glass and Guevara et al. [4], which they used to describe the changes in instantaneous firing rate of embryonic chicken heart cells.

Slices of somatosensory cortex from Sprague-Dawley rat were prepared by standard procedures [5]. We used sharp electrodes to record membrane potentials from neurons ($n = 20$) in the first third of the cortex adjacent to cerebral white matter. Intracellular injection of constant current evoked regular spiking behavior in these neurons. To simulate inhibitory input we superimposed negative rectangular current pulses of 5 ms duration at time t_i, $i = 1, 2, \ldots$ (c.f. Fig. 1) relative to the preceding spike. When we applied the current pulse soon after a spike, we observed a shortening of the interspike interval, while late application lengthened the interval, as shown in Figure 1. The effect of a stimulus arriving at time t_i after the preceding spike, on the interspike interval length T, was described in terms of phase. The phase ϕ of the applied stimulus is defined as t_i/T_0, where T_0 is the unperturbed interspike interval (c.f. Figure 1). Plotting T/T_0 versus ϕ yields the phase response curve (see Fig. 2) which shows how the interspike interval length depends on the exact arrival time of the stimulus. From the phase ϕ_i of the last stimulus, the phase of the next stimulus ϕ_{i+1} can be predicted by a Poincaré map $P: \phi_i \to \phi_{i+1}$. This claim can be confirmed from Fig. 1, which shows that the following relation holds:

$$T + t_2 = t_1 + T_s . \tag{1}$$

Dividing by the unperturbed interspike interval T_0, and using the abbreviations $\Omega = T_s/T_0$, $\phi_i = t_i/T_0$, $\phi_{i+1} = t_{i+1}/T_0$, yields

$$\phi_{i+1} = \phi_i + \Omega - T/T_0 \quad \text{(modulo 1)}. \tag{2}$$

The assumption we use in the following is that, mathematically, the oscillation is represented by a limit cycle of sufficient stability to reestablish itself after a perturbation. In this case, the perturbation during the next interspike interval can be considered as being applied novo to an unperturbed limit cycle. Regular patterns of the phases produced imply regular firing; irregular phases imply irregular firing behavior. As seen in the experiment, the set of phases produced depends strongly on the additive constant Ω, which may be interpreted as a constant phase shift. For some values of Ω irregularity occurs, for others regularity.

Reprint requests to Dr. habil. R. Stoop; Fax: (0041) 12 57 26 28.

0932-0784 / 97 / 0600-0509 $ 06.00 © – Verlag der Zeitschrift für Naturforschung, D-72027 Tübingen

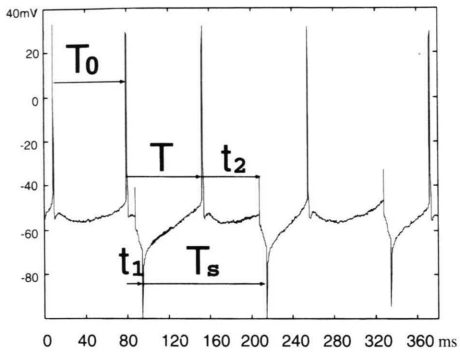

Fig. 1. Example of an experimental spike train, where the characteristic quantities T_0, T, t_1, t_2, and t_s, are indicated.

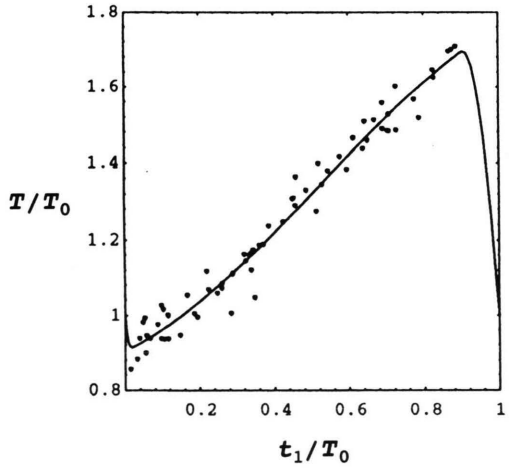

Fig. 2. Phase response curve g: $t_1 \to T$ (see Figure 1). This function expresses how the limit cycle responds to the perturbation given at the time t_1 after the last spike. When inserted in the circle-type map (2), it determines at which new phase the next perturbation accurs, given the phase of the old perturbation.

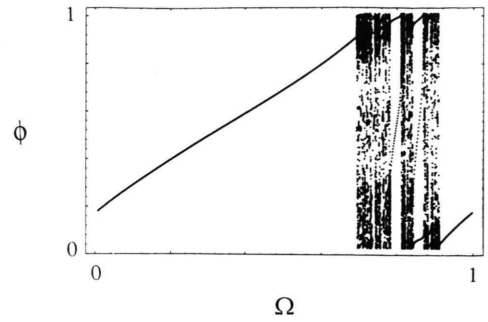

Fig. 3. Bifurcation diagram produced by the Poincaré map (2). Some periodic perturbations are performed at a fixed phase-shift Ω, before Ω is increased and again periodic perturbations are applied. In this way, each dot in the diagram represents the phase of a single perturbation. Regular firing is found at values of Ω where the phases form a discrete set. In the plot, the role of Ω is that of a bifurcation or control parameter.

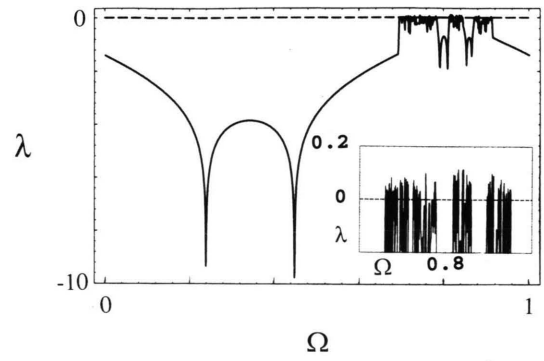

Fig. 4. Lyapunov exponents diagram. Lyapunov exponents characterize the stability properties of the motion on the perturbed limit cycle. Negative Lyapunov exponents indicate stable firing patterns, positive exponents unstable, chaotic firing patterns. Clearly, there are bands where the firing pattern is chaotic (c.f. the enlarged inset).

In the case of irregular firing behavior, the question arises whether this behavior is chaotic in nature. Two steps are required to demonstrate this. First, the iterated map is used to show that the Poincaré map actually produces chaos. Second we must supply evidence that the limit cycle behavior continues to exist under the influence of the perturbation. Plotting the Poincaré map of (2) as a function of the phase shift Ω gives rise to a bifurcation diagram [7], as shown in Figure 3. In this diagram, irregular spiking behavior is characterized by bands, which often extend over the whole range of possible phases. To prove chaotic behavior, the existence of a positive Lyapunov exponent [6] is essential. In Fig. 4 we plot the dependence of Lyapunov exponent vs. the phase shift Ω. Clearly, chaotic regions arise. We then tested the predictions made by our bifurcation diagram experimentally, by making different choices of Ω and observing the spiking pattern produced under continued perturbation. We found good agreement between predicted and experimentally observed spiking patterns [8]. As a consequence, we may state that for specific choices of the frequency shift Ω, chaotic firing can be observed.

Computer simulations of neurons [9] were used to gain insight possible biophysical mechanisms underlying the various spike patterns. We studied the dynamics of a simplified cortical pyramidal cell based on well established models described in the literature

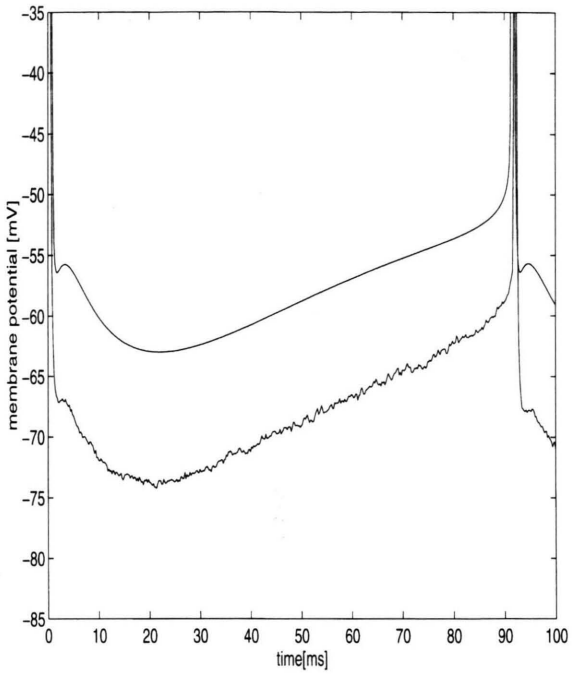

Fig. 5. Comparison between simulated (upper trace) and experimental (lower trace) membrane potential showing one interspike interval.

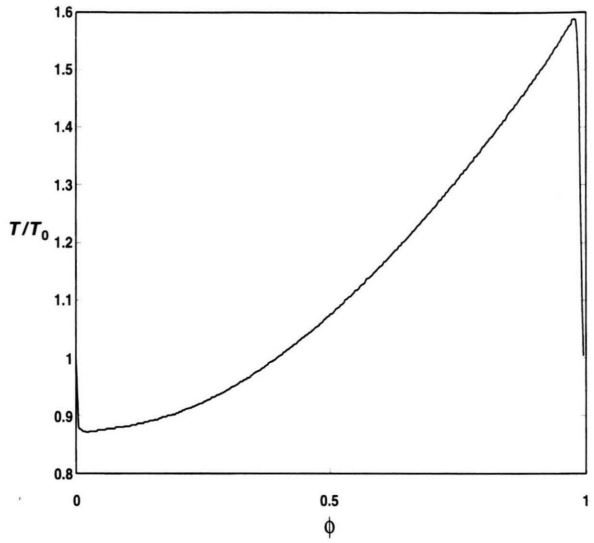

Fig. 6. Phase-response curve of the simulated cell.

[10–12]. The simulated cell consisted of a soma with eight active conductances and five passive dendritic compartments. This simplified morphology was derived from a detailed three dimensional reconstruction of a layer 5 pyramidal cell from cat primary visual cortex [13]. The current was assumed to be injected into the soma. The parameters of the ionic conductances were adjusted to reproduce the average interspike membrane voltage trajectory in response to constant current injection that was observed in our experiments. Below, we list only the parameters modified with respect to our group's previously published values [10, 11] (*G* indicates the conductance density of the current):

I_{na} (fast sodium current): inactivation time constant $= 0.3$ ms, $G_{na} = 500$ mS/cm^2; I_{dr} (delayed rectifier K^+ current): activation time constant $= 0.5$ ms; $G_{dr} = 110$ mS/cm^2; I_a (A-Type K^+ current, taken from another model of a neocortical pyramidal cell [12]): $G_a = 3$ mS/cm^2; I_m (M-type K^+ current): activation time constant $= 40$ ms, $G_m = 2.4$ mS/cm^2; I_{ahp} (Ca^{++}-dependent K^+ current): decay time constant of

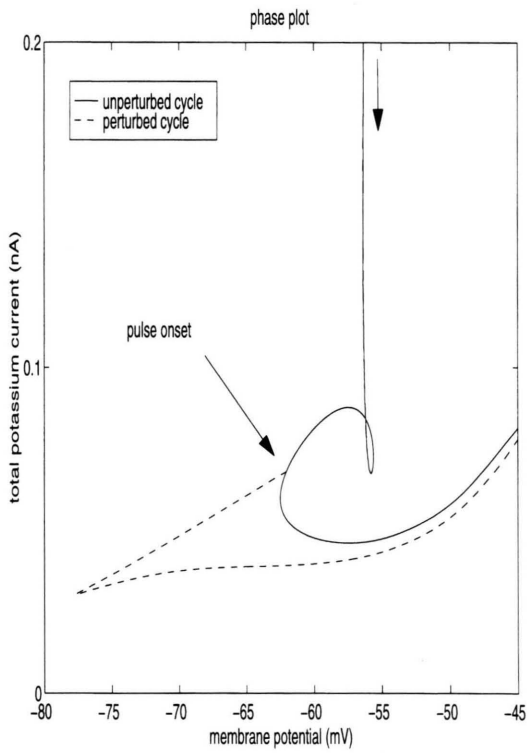

Fig. 7. Phase plot of the unperturbed and the perturbed cycles. In the phase plane of potassium current vs. membrane potential, orbits enter from the top (arrow) and exit to the right.

the intracellular $[Ca^{++}] = 40$ ms, $G_{ahp} = 80$ mS/cm^2; I_{ca} (high-threshold calcium current): $G_{ca} = 3.2$ mS/cm^2.

The behaviour of the simulated cell is in good agreement with the experimental data (see Figures 5, 6). In our simulations we found that the effect of the inhibitory pulse on the firing pattern is determined mainly by the dynamics of voltage sensitive, relatively slowly reacting K^+ channels. In agreement with previous simulations performed by Lytton and Sejnowski [14], the shortening of the perturbed interval can be accounted for by the deactivation of a voltage-gated K^+-conductance. As a consequence, the outward K^+ current decreases sufficiently to allow the cell to reach threshold earlier. Figure 7 shows a phase plane representation of this mechanism. The stimulus causes the net K^+ current to drop abruptly after the application of the pulse, mainly due to proximity of the K^+ reversal potential, and therefore a diminished driving force for the K^+-current. Subsequently, as the membrane potential is depolarized (pulled upwards) by the injected current, the K^+ current remains below the unperturbed level until the next spike. This is due to decreased activation of voltage-sensitive currents, especially the M-current [1]. The decrease in outward-current is sufficient to shorten the interspike interval, even when starting from a more negative potential. In contrast, when the same stimulus is applied later in the cycle, the interspike interval lengthens because of the time required for the membrane to recharge.

In this paper, we showed that regularly spiking neurons, when perturbed periodically with inhibitory pulses, may produce chaotic firing patterns. Our simulations indicate that these effects are determined mainly by voltage sensitive, relatively slowly reacting K^+ channels, such as the M-current. Ongoing work demonstrates that the described response of neurons is generic. That is, it is independent of special features of phase response functions of individual cells and remains qualitatively unchanged for a large range of the stimulation strength. In this sense, the reported bifurcation diagram is characteristic for the response of neurons stimulated by inhibition. The ability of the neuron to create irregularity may play an important role in observed synchronized/desynchronized activity within networks of neurons. We are currently exploring further effects introduced by more biologically motivated stimulation paradigms and their relevance for biological neuronal networks.

Acknowledgements

This work was supported by the Swiss National Science Foundation, the Maurice E. Müller Foundation, and the Helmut-Horten-Foundation.

[1] B. Hille, Ionic Channels of Excitable Membranes, Sinauer Associates, Sunderland Mass. 1992.
[2] T. H. Bullock, How Does the Brain Work? Birkhaeuser, Boston 1993.
[3] L. Glass and M. Mackey, From Clocks to Chaos, Princeton University Press, Princeton 1988.
[4] L. Glass, M. Guevara, J. Blair, and A. Shrier, Phys. Rev. A **29,** 1348 (1984).
[5] A. U. Larkman, A. Mason, and C. Blakemore, Neurosc. Res **6,** 1 (1988).
[6] R. Stoop and P. F. Meier, J. Opt. Soc. Amer. **B25,** 1037 (1988); J. Peinke, J. Parisi, O. E. Roessler, and R. Stoop, Encounter With Chaos, Springer, Berlin 1992.
[7] H. G. Schuster, Deterministic Chaos, 2nd ed.; VCH, Weinheim 1989.
[8] A more detailed analysis (including synaptic stimulation) will be presented in an extended forthcoming paper.
[9] M. Hines, Int. J. Biomed. Comp. **24,** 55 (1989); M. Hines, The Neuron Simulation Program in Neural Network Simulation Environments, J. Skrzypek ed., Kluwer, Amsterdam 1993.
[10] Ö. Bernander, R. J. Douglas, K. A. C. Martin, and C. Koch, Proc. Natl. Acad. Sci. USA **88,** 11569 (1991).
[11] Ö. Bernander, Synaptic Integration and its Control in Neocortical Pyramidal Cells, PhD thesis, California Institute of Technology, 1993.
[12] P. A. Rhodes and C. M. Gray, Neural Comput. **6,** 1086 (1994).
[13] R. J. Douglas and K. A. C. Martin, Exploring Cortical Microcircuits: A Combined Anatomical, Physiological and Computational Approach, in Single Neuron Computation, J. Davis, T. McKenna, and S. Zornetzer, eds., Academic Press, Orlando 1993.
[14] W. W. Lytton and T. J. Sejnowski, J. Neurophysiol. **66,** 1059 (1991).